Cytotoxicity of silica nanoparticles through exocytosis of von Willebrand factor and necrotic cell death in primary human endothelial cells

Alexander T. Bauer, Elwira A. Strozyk, Christian Gorzelanny, Christoph Westerhausen, Anna Desch, Matthias F. Schneider, Stefan W. Schneider

Angaben zur Veröffentlichung / Publication details:

Bauer, Alexander T., Elwira A. Strozyk, Christian Gorzelanny, Christoph Westerhausen, Anna Desch, Matthias F. Schneider, and Stefan W. Schneider. 2011. "Cytotoxicity of silica nanoparticles through exocytosis of von Willebrand factor and necrotic cell death in primary human endothelial cells." *Biomaterials* 32 (33): 8385–93. https://doi.org/10.1016/j.biomaterials.2011.07.078.

Cytotoxicity of silica nanoparticles through exocytosis of von Willebrand factor and necrotic cell death in primary human endothelial cells

Alexander T. Bauer [a,1], Elwira A. Strozyk [b,c,1], Christian Gorzelanny [a], Christoph Westerhausen [d], Anna Desch [a], Matthias F. Schneider [e], Stefan W. Schneider [a,*]

[a] Department of Dermatology, Medical Faculty Mannheim, Heidelberg University, Mannheim 68167, Germany
[b] Institute of Molecular Immunology, Helmoltz Center Munich, Munich 81377, Germany
[c] Department of Cancer Immunology, University of Medical Sciences at Great Poland Cancer Center, Poznan 61866, Poland
[d] Department of Experimental Physics I, Physics Institute, Augsburg University, Augsburg 86135, Germany
[e] Department of Mechanical Engineering, Biological Physics Group, Boston University, Boston, MA 02215, USA

1. Introduction

During the past decades the exponential growing field of Nanotechnology is considered to represent one of the key technologies of the 21st century [1,2]. Based on their unique biochemical properties nanoparticles (NP), including silicion dioxide (SiO_2) NP, are increasingly used in a broad spectrum of biomedical purposes [3]. Applications range from medical diagnostics [4], cancer therapy [5], DNA delivery [6,7] and drug delivery [8,9]. In addition nanoscaled silica are widely distributed in our environment and are manufactured on industrial scale as additives to cosmetics, paints and printer toners [10]. However, despite their widespread use in life science and industries, several epidemiological and toxicological studies link air pollution with ultrafine particles to increased cardiovascular disease [11–13]. Although the intake of NP through the gastro-intestinal tract, the skin and mucous membranes needs to be considered, inhalation is the most important route for uptake of ultrafine particles. In the lung NP induce inflammation, fibrosis and cytotoxic effects [14]. Next to the potential effects on pulmonary inflammation a number of studies have shown that NP translocate from the respiratory system towards the systemic circulation, and therefore interact with endothelial cells of the blood vessels [15,16]. The vascular endothelium with its salient location at the interface between blood and tissue and with its strongly anti-thrombotic and anti-inflammatory characteristics plays a crucial role in the process of physiological blood flow. However, different stimuli induce endothelial cell (EC) activation, switching the vessel wall to a pro-thrombotic and inflammatory surface [17]. The initial step of this process includes the exocytosis of Weibel-Palade bodies (WPBs), intracellular storage sites for inflammatory cytokines and proteins and the coagulatory protein von Willebrand factor (VWF). This glycoprotein is involved in hemostasis as a mediator of platelet adhesion to the endothelium as well as platelet–platelet aggregation [18,19].

* Corresponding author. Fax: +49 621 383 6903.
E-mail address: stefan.schneider@medma.uni-heidelberg.de (S.W. Schneider).
[1] authors contributed equally.

Almost all diseases of the cardiovascular system are associated with an altered EC function, pointed out by loosing their anti-thrombotic and anti-inflammatory function [20].

In line with these findings animal studies provide accumulating evidence that pulmonary inflammation caused by silica particles is accompanied by EC dysfunction leading to enhanced blood coagulability by activation of the clotting cascade [16,21,22]. In addition, to date several *in vitro* findings have investigated toxic effects of ultrafine silica nanomaterials. These reports suggest that silica NP are involved in production of reactive oxygen species and inflammatory responses [23–25]. Unfortunately, most previous studies focused on the acute cytotoxicity, using a wide range of different cell lines, nanoparticle concentrations and exposure times. In this regard, little is known about the impact of silica NP on physiologically relevant cell functions and interactions with the procoagulant system.

To investigate the impact of SiO_2 NP on primary human umbilical vein endothelial cells (HUVECs) *in vitro*, we examined both mitochondrial activity as well as membrane leakage to characterize NP-induced cytotoxicity. In an attempt to further analyze the underlying pathways of cell death mediated by silica particles, FACS analysis and caspase 3/7 activity measurements were performed. Procoagulatory effects of NP and thus VWF release and EC activation were analyzed by immunofluorescence stainings. Furthermore, to gain a closer insight into NP-cell interactions we determined cellular uptake and subcellular localization in HUVECs by high resolution microscopy techniques and correlated these data with observed cytotoxic effects. Finally, the effect on cell migration and proliferation was tested.

2. Materials and methods

2.1. Particles preparation and characterization

Plain (unlabeled) and with a monofunctional perylene derivate (MPD) surface-labeled silica nanoparticles with particle diameters between 16 nm and 310 nm were kindly provided from Armin Reller of the Department of Solid State Chemistry (University of Augsburg, Germany). These particles were produced by a modified Stöber process and characterized as described before [26]. Particles were suspended in sterile water at a concentration of 3 mg/ml and always sonicated for 3 min and vortexed immediately before addition to culture medium to minimize their aggregation.

2.2. In vitro experiments

2.2.1. Cell culture

HUVECs were isolated using collagenase and grown in Endothelial Cell Growth Medium (PromoCell, Heidelberg, Germany) supplemented with 10% heat inactivated fetal calf serum (FCS), 1% penicillin and streptomycin, 5 U/ml heparin (Biochrom, Berlin, Germany) and 1% growth supplement derived from bovine retina as described [27]. Cells were maintained at 37 °C with 5% CO_2 and cultivated maximally up to the third passage.

2.2.2. Stimulation of HUVECs with nanoparticles

For viability tests HUVECs were grown in gelatin-coated 96 well plates (Becton Dickinson, Meylan Cedex, France) for 24 h. For each time point (24 h, 48 h), 15000 and 10000 cells were seeded into every well of the 96 well plates in triplicate. HUVECs were stimulated with the described particle suspensions in a dose of 1000, 15000 and 30000 NP per cell in 100 μl medium without additives for 24–48 h. Untreated cells or cells incubated with the corresponding concentrations of ultrapure water served as controls.

2.2.3. MTT-assay

After exposure to the SiO_2 NP 100 μl of the medium was removed and toxicity was determined using the 3-(4,5-dimethylthiazol-2-yl)-2,5-diphenyltetrazolium

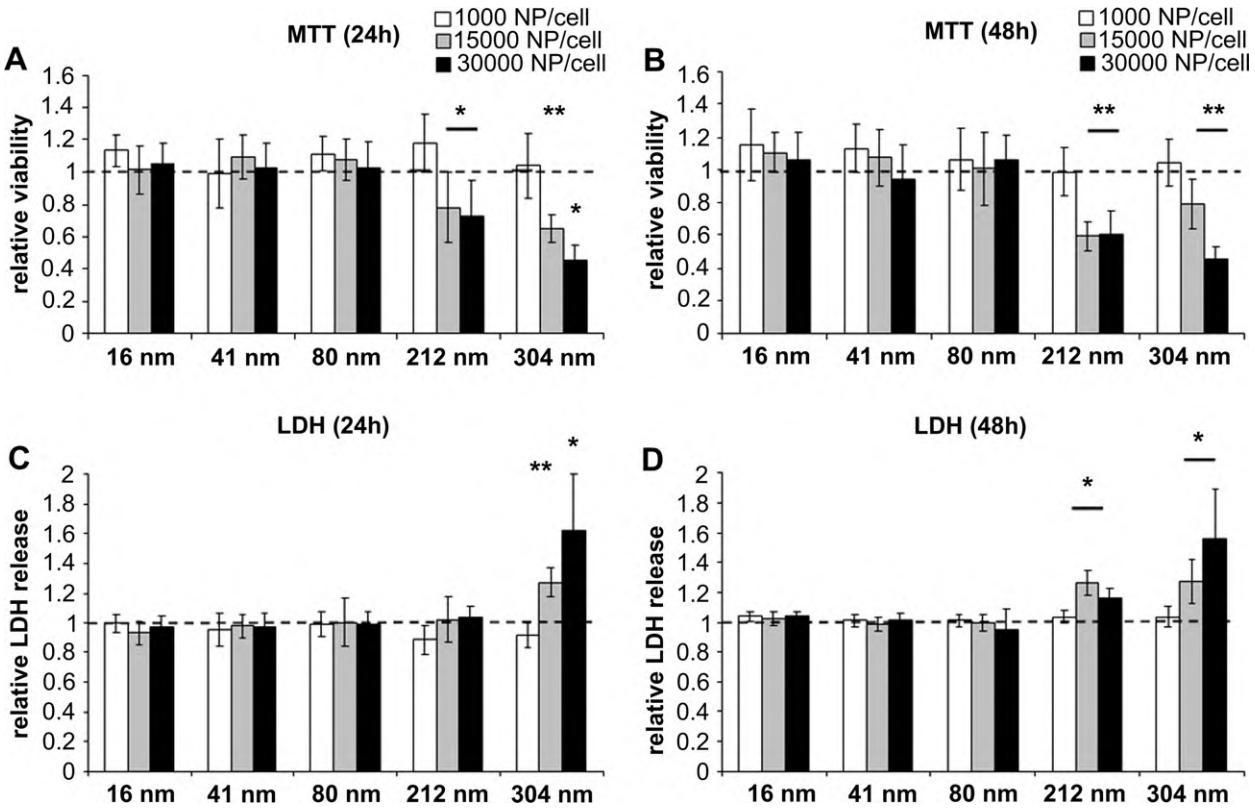

Fig. 1. Viability of human endothelial cells after exposure to silica Nanoparticles. Primary Human umbilical vein endothelial cells (HUVECs) were incubatated with SiO_2 NP with a size ranging from 16 nm to 304 nm and cytotoxicity was assessed by MTT and LDH assays. Quantification and normalization to untreated controls (dotted line) showed a size and concentration dependent reduction of mitochondrial activity after 24 h (A) and 48 h (B) of exposure. Data represent mean ± standard deviation (SD) from three independent experiments ($n = 6–9$). (C, D) Quantification of membrane leakage indicates a size- and dose-dependent membrane leakage after exposure to NP. Data are expressed at means ± SD of at least three independent experiments with pooled triplicates (*$p < 0.05$, **$p < 0.01$).

bromide (MTT) reduction assay [28]. The absorbances were measured at 570 nm and expressed as relative values compared with untreated negative control.

2.2.4. LDH-assay

Membrane leakage was quantified by detection of Lactate dehydrogenase in the removed supernatant [29] using LDH assay kit (Roche, Mannheim, Germany). The absorbance was measured at a wavelength of 490 nm by using Synergy 2 multi-mode microplate Reader (BioTek, Winooski, USA) and results are presented as relative values compared to control.

2.2.5. Fluorescence-activated cell sorting

To distinguish between viable and non-viable cells, we focused on a fluorescence-based method using propidium iodide (PI). After exposure to 15000 silica NP/cell for 24 h cells were harvested with accutase (PAA, Pasching, Austria), washed with PBS and fixed in 70% ethanol for at least 1 h at 4 °C. Subsequently they were centrifuged, resuspended with PBS and incubated with 50 μg/ml PI for 5 min in the dark. The number of dead versus living cells was analyzed using FACS SLRII and Diva Software. WinMDI software was used to analyze the events.

2.2.6. Analysis of caspase activity

To define wheter observed cell death results from apoptosis, Caspase Glo 3/7 assay (Promega, Heidelberg, Germany) was performed according to the directions of the supplier. HUVECs were seeded in white 96 well plates (15000 cells/well) in cell culture medium and were allowed to attach overnight. For stimulation with NP 100 μl of the medium was removed and replaced with 100 μl medium containing the NP without additives. Apoptosis of HUVECs was induced as positive control by 1 μmol/L staurosporine (Sigma, Steinheim, Germany). After treatment 100 μl culture medium was replaced by Glo 3/7 reaction buffer and was incubated for 30 min at 37 °C. Luminiscence was measured by Synergy 2 multi-mode microplate Reader (BioTek, Winooski, USA). The results were expressed as relative fluorescence compared to the control.

2.2.7. Immunofluorescence

HUVECs were grown on gelatine-coated coverslips in a 12 well plate (150000 cells/well), followed by an incubation of 24 h. After incubation cells were stimulated for 15 min, 2 h or 24 h with the NP (15000−30000/cell). Coverslips were then fixed in ice-cold methanol for 30 min, washed with HEPES and blocked with 2% bovine serum albumin (BSA) in an incubation buffer (0.1% BSA in HEPES-buffered Ringer solution (HBRS) consisting of 140 mM NaCl, 5 mM KCl, 1 mM $MgCl_2$; 1 mM $CaCl_2$, 5 mM glucose and 10 mM HEPES; 0.3% Triton X-100) for 1 h at room temperature. Incubation with the primary antibody mouse anti-human CD31 or rabbit anti-human VWF (DakoCytomation, Glostrup, Denmark) was performed with a dilution of 1:40 or 1:150 in incubation buffer for 1h at room temperature. After washing cells were incubated with secondary FITC-conjugated goat anti-mouse or goat anti-rabbit IgG antibodies (BD Pharmingen, San Diego, CA) diluted 1:400 in incubation buffer at room temperature for 1 h. Nuclei were stained with 4,6-diamidino-2-phenylindole (DAPI) diluted 1:10000 in phosphate buffered saline (PBS) for 10 min. Finally, coverslips were embedded with mowiol−glycol solution with freshly added 50 mg/ml DABCO (1.4- diazabicyclo-[2.2.2] octane; Sigma-Aldrich, Taufkirchen, Germany). Confocal microscopy was acquired using a confocal laser scanning microscope DMIRE2 (Leica, Wetzlar, Germany) under a 60× oil-immersion objective and data were analyzed by ImageJ.

2.2.8. Atomic force microscopy

For atomic force microscopy (AFM) cells were fixed with 2% Formaldehyde in PBS after incubation with NP, without any preparation or manipulation of the sample. AFM (The NanoWizard, JPK Instruments, Berlin, Germany) analysis was performed by contact mode in PBS. The applied force in contact mode was 0.5 nN with a scan rate of 1 Hz. The spring constant of the cantilever (MLCT-AUHW cantilevers, Veeco Metrology Group, Santa Barbara, CA, USA) was 0.01 N/m.

2.2.9. Wound healing assay

For the study of regeneration and migration upon NP Stimulation, HUVECs were cultured in a μ-Dish with Culture-Inserts (Ibidi, Martinsried, Germany) at a density of 35 x 10^3 cells/well and incubated at 37 °C for 24 h. Culture-Inserts were removed with sterile tweezers and cells were incubated with NP (15000/cell). After different time intervals of incubation the samples were examined microscopically (Axiovert 100; Zeiss, Jena, Germany).

2.3. Statistical analysis

For statistical analyses, the unpaired Student's *t*-test was used. Values were expressed as the mean ± s.d. Results were considered as statistically different at $P < 0.05$.

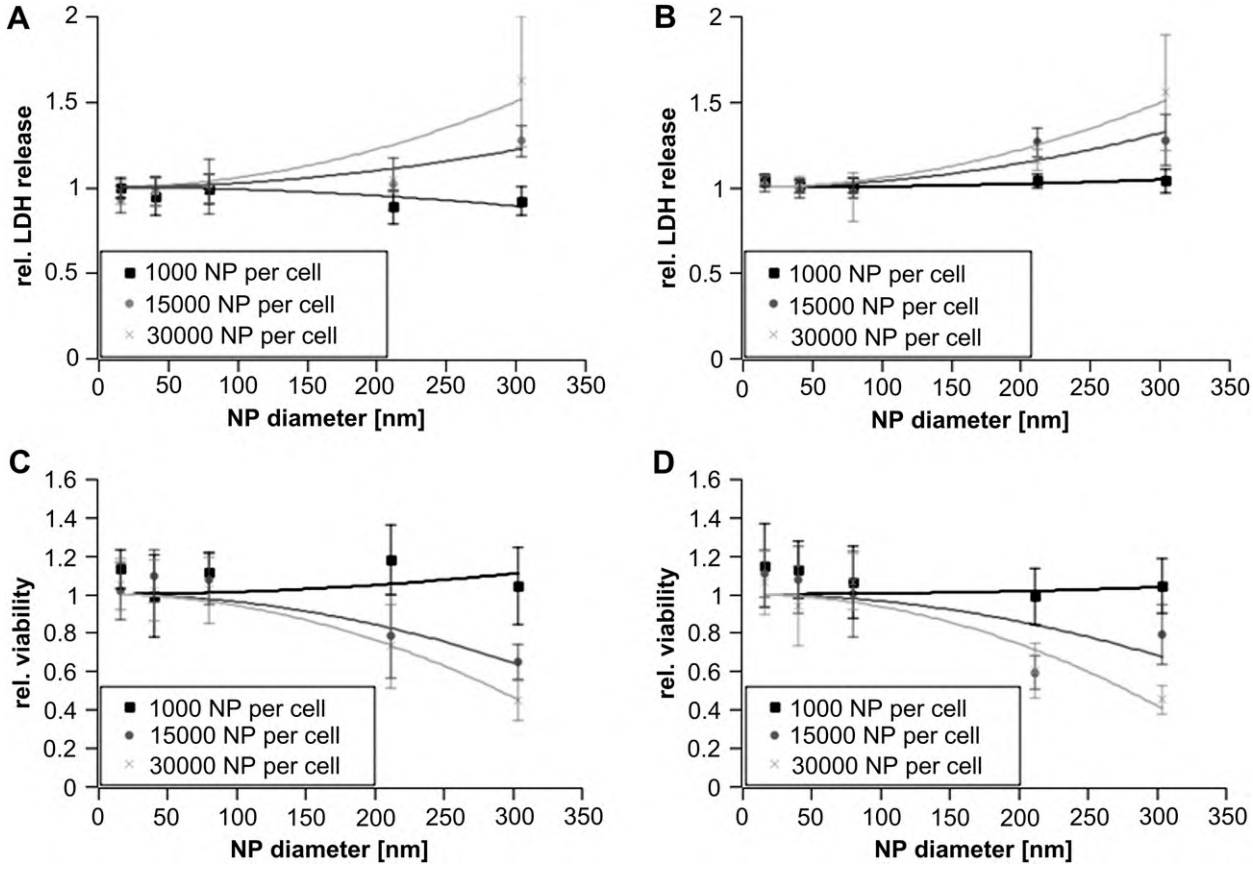

Fig. 2. Quadratic fits to the cytotoxicity quantities of LDH and MTT assays. A, B: LDH assays after 24h and 48h exposure time. C, D: MTT assays after 24h and 48h exposure time. In all cases the quantities of toxicity can be fitted by a quadratic function of the NP diameter. The highest concentration 60.000 particles per cell were only measured for the biggest particles and we simply chose the parameter *a* to fit this single point.

3. Results

3.1. Dose- and size-dependent cytotoxicity of silica nanoparticles

In order to evaluate possible toxic effects of SiO_2 NP on primary human ECs, cytotoxicity was assessed using the MTT reduction method and the LDH assays. Cells were exposed to different concentrations (1000 NP/cell; 15000 NP/cell; 30000 NP/cell) of NP with diameters between 16 nm and 304 nm for 24 h and 48 h. As shown in Fig. 1, the cytotoxicity induced by silica NP increased in a significant size and dose-dependent manner. After exposure of 24 h, mitochondrial activity significantly decreased upon incubation of NP with diameters between 212 nm and 304 nm. However, NP with a diameter of 80 nm or less showed no cytotoxicity within the same particle concentrations (Fig. 1A). Compared to the untreated control (dotted line) metabolic activity was reduced by more than 40% upon incubation with SiO_2 particles in size of 304 nm at concentrations of 15000 NP/cell (Fig. 1A). This reduction of NP-induced viability decreased to 45% at 30000 NP/cell, indicative for a dose-dependent cytotoxicity (Fig. 1A). Furthermore, this effect strongly correlated with increased membrane damage, measured by LDH release and, therefore is indicative for cell death (Fig. 1C). Regarding the kinetics of NP-induced toxicity in ECs, we could not find significant changes comparing the exposure times 24 h and 48 h (Fig. 1B, D).

To quantify the cytotoxicity of the used NP we take into regard that smaller particles have a large ratio of surface to weight. Thus, our data indicate that the surface area is the most important parameter determining toxicities of SiO_2 particles as we will show in this section.

The concentration of NP in the MTT and LDH assay represents the number of particles per cell. Hence, if the cytotoxicity is proportional to the surface area, the quantities determined by these assays (here simply indicated by the letter F) should fit a quadratic function of the diameter d:

$$F(d) = 1 + \beta c_p d^2 \pi = 1 + \alpha c_p d^2 \quad (1)$$

where c_p is the number of particles per cell and α and β interaction parameters.

For all cases our data matches a function of the form of Equ. (1) (Fig. 2). In both, LDH and MTT assays as well as after 24 h and after 48 h the relative cytotoxicity value can be fitted with a quadratic function F(d) (Fig. 3). The fit parameter α, although held free during the fit, is nearly constant for 15000 to 60000 NP per cell with α approximately 1,8 10^{-10} nm^{-2}, which demonstrates that the surface area and not the mass of NP are responsible for cytotoxicity.

Due to the documented cytotoxicity associated with NP of 304 nm in diameter, only these NP were used in subsequent cell death studies. In order to investigate uptake and subcellular localization, fluorochrome (perylene)-labeled NP were used. Since the potential cytoxicity of NP is related by their surface charge and chemical composition, we next compared the effect on EC viability of particles with and without perylene functionalization (Fig. 4). MTT and LDH results showed that fluorescent labeled particles of 310 nm exhibit comparable effects on cell viability compared to unlabeled NP after 24 h (Fig. 4A) and 48 h (Fig. 4 B). Similar results were obtained from particles ranging from a diameter from 15 nm to 230 nm (data not shown) indicating that our surface functionalization with perylene does not influence cytotoxicity of the used SiO_2 NP.

3.2. Mechanism of cell death

To further analyze the cytotoxic effects caused by silica NP, cell death of HUVECs was quantified by incubation with propidium iodide (PI), staining nuclear DNA. Assuming that dead cells exclude parts of the labeled DNA due to membrane leakage, measured fluorescence allows to distinguish between dead and viable cells. After 24 h of exposure to 15000 NP/cells cell death was assessed by flow cytometry (Fig. 5A,B). In accordance to the MTT and LDH data, quantitative analysis revealed that EC exposure to silica particles resulted in a significant 4.36 ± 0.97-fold increase of cell death

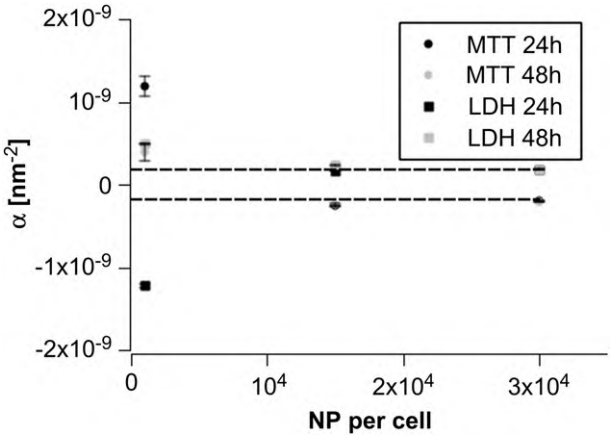

Fig. 3. The interaction parameter α is plotted versus the number of particles per cell. As a guide for the eye the constants $y = \pm 1{,}8 * 10^{-10}$ nm^{-2} are plotted as dashed lines. Note: For the lowest concentration (1000 NP per cell) the standard deviation of the cytotoxicity marker is to high to extract a reliable value for the parameter α.

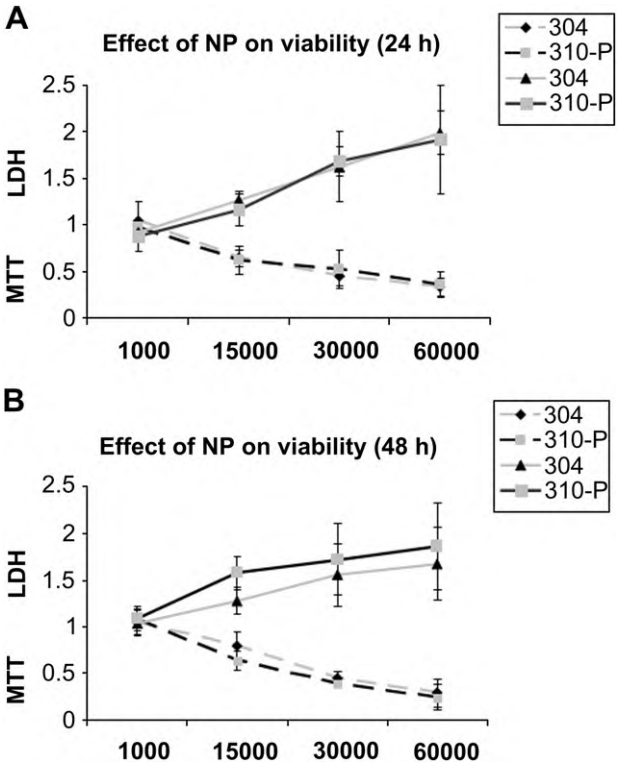

Fig. 4. Surface functionalization of silica nanoparticles does not change cytotoxicity. Effect of particles with a size of 304 nm and perylene-labeled SiO_2 NP (310-P) on viability of endothelial cells was analyzed by MTT and LDH measurements. Quantitative analysis revealed a strong correlation between reduced metabolic activity (grey and black dotted lines) and membrane damage followed by LDH release (grey and black lines). Cytotoxicity increased within the first 24 h of exposure (A) without showing further elevation after 48 h (B). Particles with surface modifications (black lines) showed no changed toxicity compared to the unlabeled controls (grey lines). Values are mean ± SD from three independent experiments.

compared to untreated ECs (Fig. 5B). To distinguish whether cell toxicity results from necrosis or apoptosis, we next analyzed activiation of caspases 3/7, key players in the apoptotic pathway (Fig. 5 C,D). Staurosporine-induced apoptosis, as a positive control, showed a strong increase of caspases 3/7 activities to more than 300% after 6 h and was still increased almost 2-fold after an incubation time of 24 h. In contrast, stimulation of ECs with different amounts of 304 nm sized NP, did not alter caspase 3/7 activity neither after 6 h (Fig. 5C) nor after 24 h (Fig. 5D). Therefore, apoptosis can be excluded and cytotoxicity of silica NP in HUVECs is related to necrotic processes.

3.3. Endothelial cell activation

EC activation is followed by acute exocytosis of vasoactive VWF, a marker of procoagolatory response [30,31]. To determine whether well defined SiO_2 NP [26] induce an activation of coagulation cascades in primary human ECs, we analyzed the release of VWF in the presence of NP (Fig. 6). For our experiments we stimulated HUVECs with perylene-labeled particles with a diameter of 310 nm for 15 min and 24 h. Furthermore, we stimulated the cells with or without addition of histamine (25 μM) and EC activation was analyzed by immunofluorescence stainings against VWF. As shown in Fig. 6, untreated control cells show VWF stored in WPBs (Fig. 6A). By contrast, 15 min of stimulation with histamine induced exocytosis of WPBs associated with the formation of ULVWF on the EC surface (Fig. 6B; arrow). After NP incubation for 15 min, no enhanced VWF fiber formation was detected in HUVECs, indicative for low EC activation in comparison to costimulation with the known secretagogues histamine (Fig. 6C). As shown in Fig. 1C, fluochrome-labeled NP (red) showed a diffuse distribution on the coverslip without any signs of cellular uptake. By contrast, after incubation of 24h NP were detected inside the cell, correlating with enhanced VWF release and VWF fiber formation (Fig. 6D; arrow). Thus, we concluded that *in vitro* treatment of primary human ECs with NP is not a strong inducer of acute EC activation. However, VWF fibers were visible after stimulation for 24 h, demonstrating a direct effect of NP on ECs.

3.4. Subcellular localization of silica nanoparticles

To gain closer mechanistic insight into SiO_2 NP-induced biological effects, we tested whether NP-induced necrosis depends on cellular uptake. Changes in the morphology of ECs were analyzed after 24 h of incubation with perylene-labeled NP with a diameter of 310 nm by using phase-contrast microscopy. In the case of 15000 NP/cell, effect on the viability of ECs was observed by formation of vacuoles in the cytoplasm of treated cells. Moreover, cell margins appeared irregular with disrupted cell–cell contacts compared to the control (data not shown). Cellular uptake and subcellular localization were analyzed by high resolution scanning confocal microscopy and atomic force microscopy at different time points upon stimulation with NP (Fig. 7). AFM images, as shown in Fig. 7, display the cellular destination of SiO_2 particles after 2 h of incubation. Following NP adhesion to the luminal endothelial cell membrane (Fig. 7A, red dots), all particles entered the cytoplasm within 24 h of incubation (Fig. 7B, red dots). Confocal microscopy analysis (Fig. 7C) and subsequent three-dimensional reconstructions (Fig. 7D) of vascular ECs revealed that fluochrome-labeled particles are located inside the cell in the perinuclear regions.

3.5. Impact of silica nanoparticles on cell migration

Endothelial cell migration is involved in many physiological processes such as remodeling and formation of new blood vessels, and as well as in pathophysiological conditions such as inflammation, tumor growth and metastasis formation [32]. To investigate

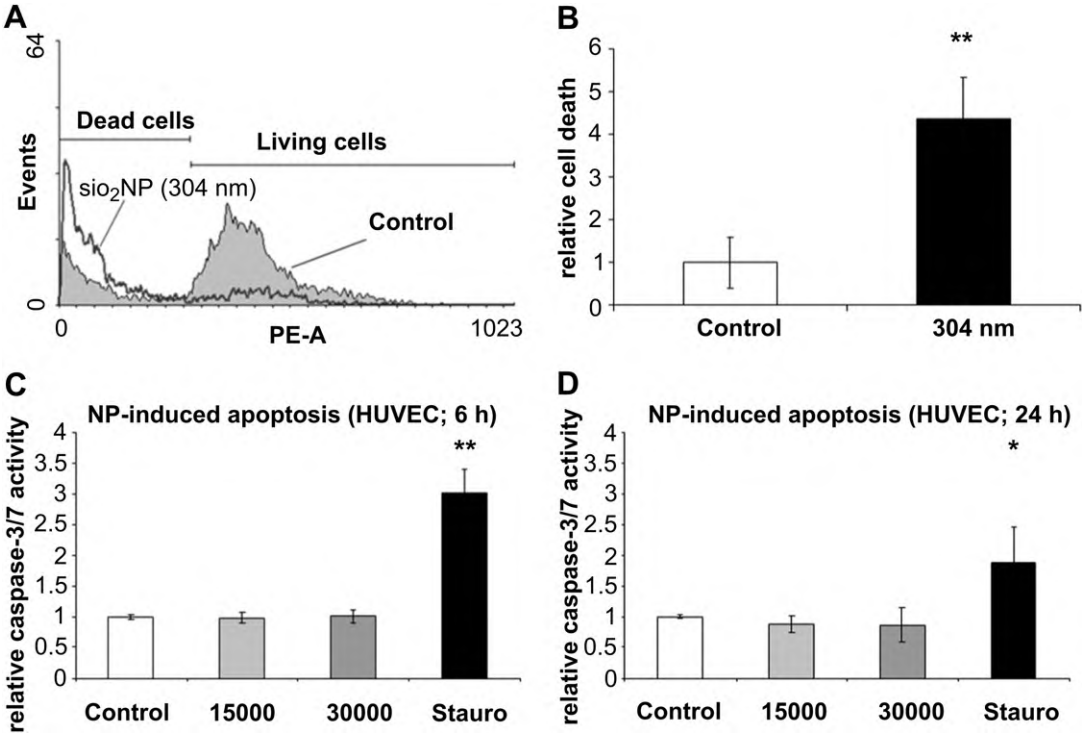

Fig. 5. Silica nanoparticles induce necrosis in human endothelial cells. Primary human umbilical vein endothelial cells (HUVECs) were exposed to SiO_2 NP with a size of 304 nm at a dose of 15000 NP/cell for 24 h. Cell viability was assesses by propidium iodide (PI) staining. FACS analysis (A) and quantitative analysis (B) showed that cell viability was significantly reduced by NP exposure. Apoptosis was assessed by the caspase 3/7 activity using a colometric caspase-specific substrate and treatment with Staurosporin (Stauro) served as positive control. Results indicate no NP-induced apoptotic cell death neither after 6 h (C) nor after 24 h (D) compared to the control group. Results represent the means of three independent experiments for FACS ($n = 4$) and for caspase 3/7 activity ($n = 6$) and error bars represent the standard error of the mean ($^*p < 0.05$, $^{**}p < 0.01$).

the consequence of SiO_2 uptake on EC migration, a wound healing assay was performed (Fig. 8). Untreated control cells showed a high migration already after 16h and a confluent EC layer was reached within 24 h (Fig. 8). On the contrary, HUVECs treated with 304 nm and 310 nm sized particles showed impaired cell migration activity and an almost blockage of cell migration after 16 h of NP incubation (Fig. 8). By contrast to the untreated control, NP treated HUVECs were not confluent even after 24 h, concluding that internalization of NP affect both cell migration and proliferation.

4. Discussion

In the present study we show that (1) SiO_2 particles-induced cytotoxicity is surface area-dependent and mediated by necrotic pathways, (2) silica NP per se are not able to activate ECs within minutes, (3) NP-induced cell disruption after stimulation of 24 h leads to WPB exocytosis followed by the release of VWF and the formation of ULVWF and (4) perinuclear localization is associated with cell death and impairs cell migration and proliferation. To the best of our knowledge, this is the first *in vitro* study showing the impact of NP on WPB exocytosis in primary human ECs by analyzing ULVWF release, pathways of cytotoxicity and effects on cell migration in correlation to NP uptake. An increasing body of evidence indicates an elevated risk of cardiovascular and pulmonary diseases upon exposure to air pollution with nanomaterials [11,14,21]. In contrast to previous studies, indicating that NP are capable of producing inflammatory stimulation [33] and reactive oxygen species (ROS) [24,34], leading to the development of cardiovascular diseases, our findings support the hypothesis that exposure to silica nanomaterials causes endothelial dysfunction, VWF release and EC necrosis, thereby generating a procoagulant condition.

4.1. SiO_2 nanoparticle-induced cytotoxicity is size-dependent

Size-dependent cytotoxicity has been well documented and it is generally accepted that the smaller a particle, the greater its toxicity [14,35]. However, the results on the effect of silica particles with different diameters are conflicting. It was previously reported that small particles with diameters of 15 nm and 46 nm induced severe cellular damage in lung cancer cells [24]. Similar results were obtained from NP with sizes of 21 nm and 48 nm in myocardial cells [36]. This is consistent with recent data, showing that spherical silica particles with diameters of 60 nm or more caused very low cellular damage in endothelial-like EAHY926 cells, whereas exposure to 15 nm NP resulted in cell damage and a decrease in cell survival [37]. However, Zhang and coworker demonstrated that smaller SiO_2 particles showed less cytotoxicity in HepG2 cells compared to bigger sized NP [38]. Furthermore, exposure to NP with surface modification was associated with low or no cytotoxicity [39]. We found that particles larger than 212 nm induce significant increased toxicity in HUVECs in the dosage of 15000-30000 NP/cell, whereas any effects on viability could be detected for particles with a size ranging from 16 nm to 80 nm (Fig. 1,4). The discrepancies between observed cytotoxicity in different studies might depend on the wide range of NP concentrations, exposure times and different metabolic activity or uptake efficiency of the cell types being used [40,41]. In the results section we already showed that the strength of cytoxicity effects is proportional to the overall surface area of the added NP. But we'd like to point out that we do not present a master equation for cytotoxicity effects for all concentrations of NP. Rather we show that it is the surface area of SiO_2 NP that is the crucial parameter of toxicity and not its volume, mass or concentration. Indeed, assuming a cubic dependence between cytotoxicity and diameter ($\sim$volume or mass), the fits exhibit significantly higher deviations and do not deliver a constant α, i.e. the data appear as if changes in interaction take place (data not shown). Especially in light of the inheterogenious effects of NP reported, this analysis strongly suggests, that when studying the impact of NP on cells it is important to consider the effective area and not only size and concentration as a variable. Otherwise, geometric effects are obscured and can be easily misinterpreted as changes in interactions between NP and cells.

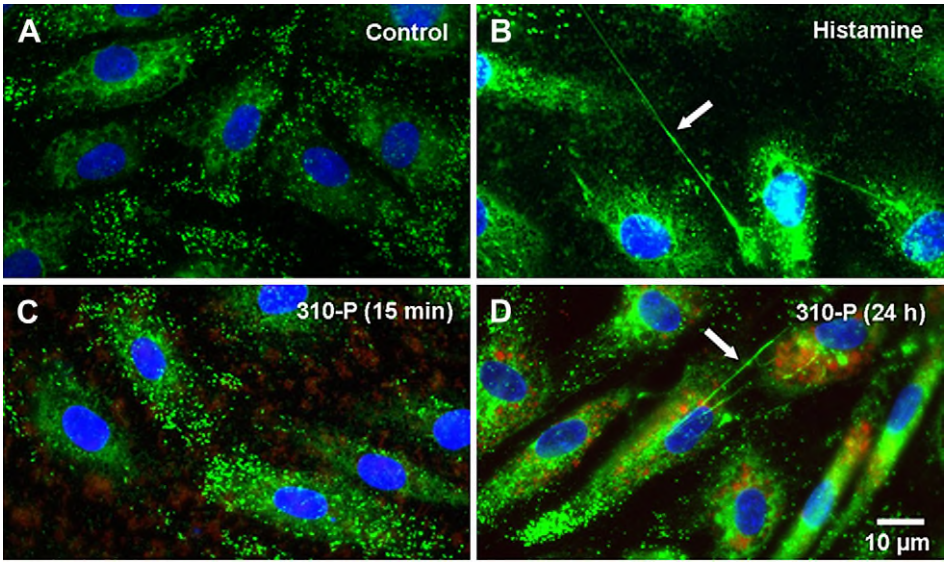

Fig. 6. Silica nanoparticles induce endothelial cell activation. Primary Human Umbilical Vein Endothelial Cells (HUVECs) were incubated with perylene-labeled (P) SiO_2 Nanoparticles (NP) with a size of 310 nm in a dose of 30000 NP/cell for 15 min, 24 h or remained untreated. HUVECs were stained with von Willebrand Factor (VWF; green) and nuclei were stained with 4,6-diamidino-2-phenylindole (DAPI). Subcellular distribution of NP is shown in red. (A) Control cells showed an intracellular localization of VWF in Weibel-Palade bodies. (B) 15 min-treatment with histamine (25 µM) induces EC activation followed by the release of VWF and fiber formation (arrow). NP show diffuse distribution (red) after incubation of 15 min without any signs of VWF release and ultra large VWF fiber (ULVWF) formation on the cell surface (C). (D) NP are located inside the cell after exposure of 24 h (red). This correlated with an exocytosis of WPBs and the formation of VWF ultralarge fibers (arrow). Representative pictures of at least two independent experiments are shown.

Thus, although the cytotoxic effects of silica NP seem to be context dependent, our results of cell death analysis are in line with ealier findings. Treating ECs with NP with a diameter of about 300 nm for 24 h, our data point towards necrosis and not apoptosis. Consistent with MTT values and LDH release, a significant increase of PI positive cells was noted at concentrations upon 15000 NP/cell (Fig. 5 A, B), indicating necrotic cell death. Induction of necrosis by SiO_2 particles have been observed in different cell types [41,42]. Others have also reported endothelial dysfunction after stimulation of silica NP causing both, necrosis and apoptosis [34]. However, as caspase 3/7 activity was not altered (Fig. 5 C, D), apoptosis could be excluded. Taken together, our data indicate, that exposure to SiO_2 causes cytotoxicity directly leading to necrosis and that the cytotoxicity of silica NP is proportional to the total surface area of added particles.

4.2. *SiO_2 nanoparticles induce von Willebrand factor release from endothelial cells*

Several data and reports from animal studies suggest that both, pulmonary inflammation [14,25,43], as well as thrombosis [21] is mediated by SiO_2 NP-induced impairment of EC function and activation of the coagulatory pathway. Furthermore, silica NP are strong inducers of oxidative stress and inflammatory responses in various cell types including epithelial cells, fibroblasts, macrophages and endothelial cells [24,34,38,44]. Data from *in vivo* intratracheal instillation of NP support the hypothesis that silica NP induce lung inflammation and platelets aggregation that may initiate thrombotic events [21,22]. Assessing the procoagulant properties of NP with diameters of about 300 nm, we were able to demonstrate that NP do not immediately activate ECs measured by VWF release (Fig. 6). Our own results strengthen the idea that the impact of NP on ECs is directly correlated with their cellular uptake as the particles induce VWF release and fiber formation upon 24 h (Fig. 6 D). In this context, it has been suggested that apoptotic vascular ECs become procoagulant due to disturbances of membrane integrity [45,46]. Therefore, we postulate that necrotic cells, next to VWF release, generate a procoagulant environment by membrane damage, release of cytosolic contents and exposure of subendothelial matrix containing matrix VWF and collagen.

4.3. *Cytotoxicity of SiO_2 nanoparticles depends on cellular uptake and subcellular destination*

Although there is good evidence that internalization and intracellular distribution of SiO_2 NP alter physiological relevant cellular events [47], the exact mechanisms of NP-induced endothelial dysfunction leading to a pro-coagulant state remain to be

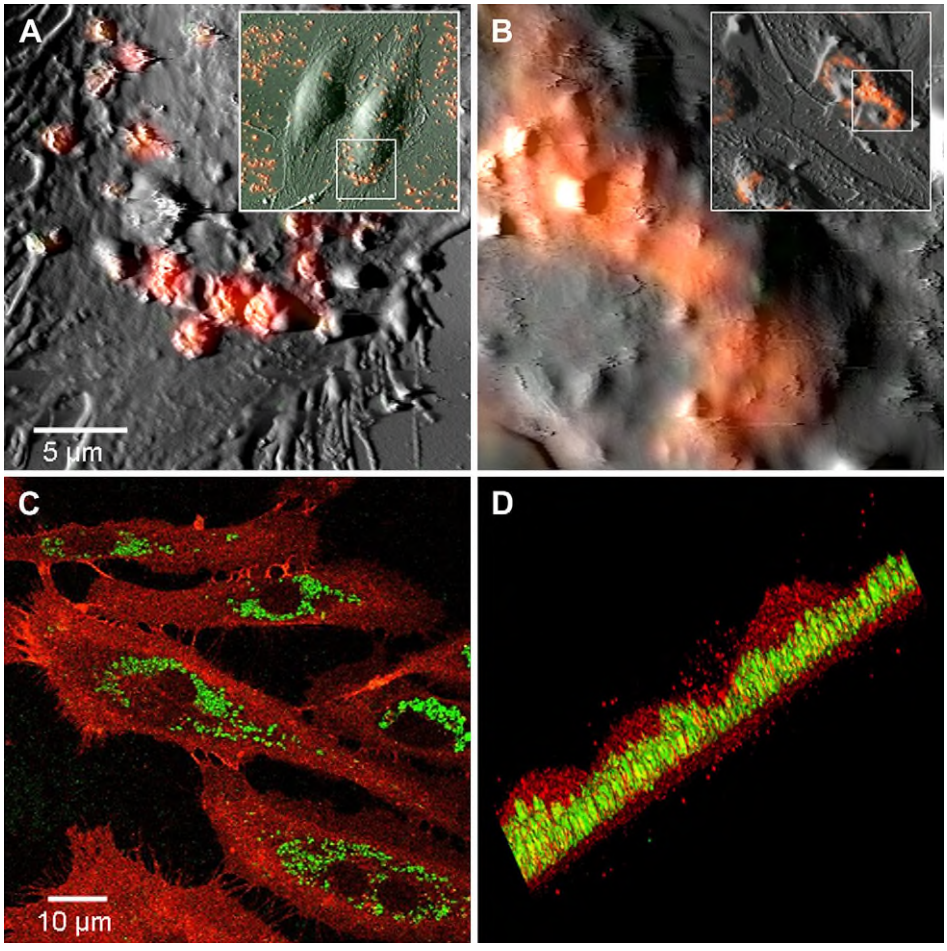

Fig. 7. Perinuclear localization of silica nanoparticles in human endothelial cells. Primary human umbilical vein endothelial cells (HUVECs) were incubatated with perylene (P)-labeled SiO_2 NP with a size of 310 nm at a dose of 15000 NP/cell. Three-dimensional atomic force microscopy (AFM) was combined with fluorescence microscopy. Whereas, NP were visible on the cell membrane outside the cells after exposure for 2h (A), the surface of the cells after incubation of 24 h is characterized by homogeneous distribution of only small humps, indicating the cellular uptake of NP (B). HUVECs were co-stained with platelet endothelial cell adhesion molecule-1 (Pecam-1; CD31; red) and subcellular location of NP (green) after exposure for 24 h was visualized by scanning confocal fluorescence microscopy (C). Three-dimensional reconstruction after confocal microscopy demonstrates localization of NP within the cells (D).

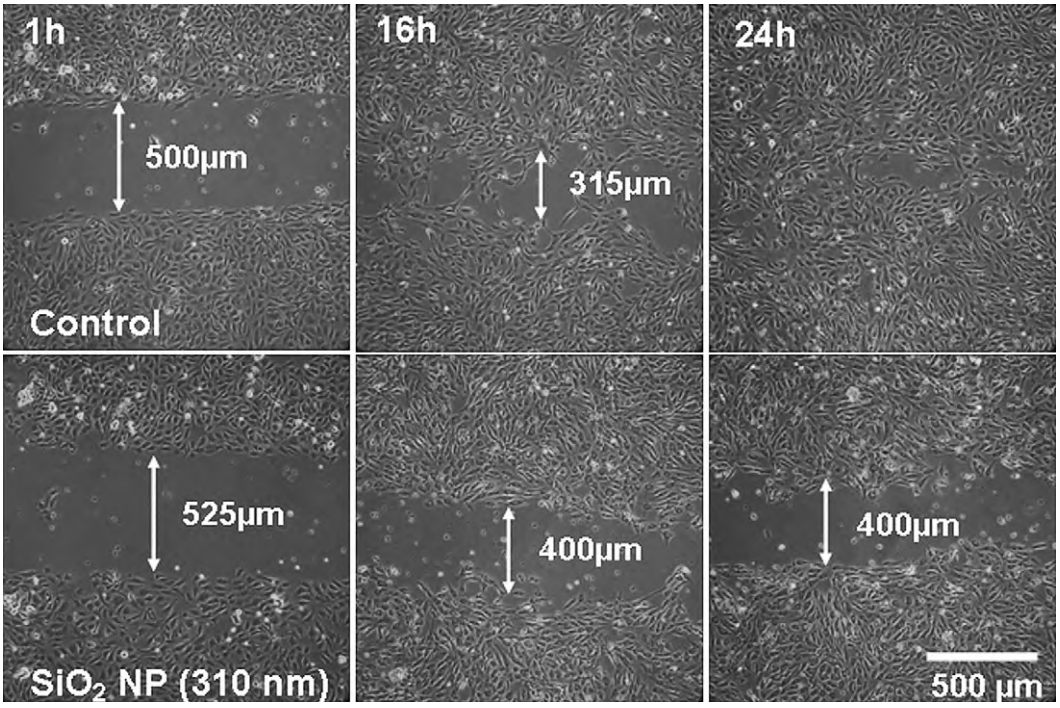

Fig. 8. Silica nanoparticles affect migration and proliferation of human endothelial cells. Primary human umbilical vein endothelial cells (HUVECs) were incubatated with the particle suspension (304 nm and 310 nm) in a dose of 15000 NP/cell and were examined microscopically at different incubation times (1 h, 16 h, 24 h). Untreated cells served as controls. Representative pictures of both groups show reduced cell migration and proliferation after treatment with nanoparticles ($n = 3$ of three independent experiments).

determined. Our results strongly indicate a direct correlation between subcellular distribution of NP and cytotoxicity as (1) perinuclear localization resulted in specific increase of necrotic cell death and (2) impaired EC migration and proliferation. It is well known that the internalization process is actin-dependent [48], including clathrin-mediated endocytosis, pinocytosis and caveolae-dependend pathways [49]. Earlier studies using epithelial cells revealed that fluorescent labeled SiO_2 NP sized between 40 nm and 70 nm penetrate the nucleus leading to intranuclear aggregates that inhibit replication, transcription and cell proliferation. In line with our findings (Fig. 7) the authors showed that larger sized particles (0.2 µm–5 µm) accumulated around the nucleus [41]. In addition, another report demonstrated that porous silicon-based microparticles were located in the perinuclear region of HUVECs after phagocytosis, indicating endocytic transport via microtubules in HUVECs [50]. An earlier study observed a higher migration rate in human melanoma cells after stimulation with mesoporous SiO_2 NP [51]. By contrast, others found inhibitory effects of silica NP on migration and proliferation of human dermal fibroblasts by using wound healing assay [38]. Another report showed toxic responses mediated by particle-induced G1 phase arrest, triggering toxic response by generation of oxidative stress [36]. Taken together, our results (Fig. 8) that are consistent with cytotoxicity data (Fig. 1,4) strengthen the idea that SiO_2 NP attenuate both cell migration and proliferation upon cellular uptake and perinuclear accumulation.

5. Conclusions

In summary, the current toxicologal evidence is clearly supportive for vascular effects arising from exposure to particles in the nanoscale. We have shown that SiO_2 NP exert toxic and therefore procoagulatory effects on ECs. The here presented mechanistic pathway could act through cellular uptake of NP, which leads to membrane damage, necrotic cell death and the subsequent release of intracellular contents. This mechanism leading to the release of procoagulant factors (VWF release) and necrotic EC exposing subendothelial matrix proteins may add informations to the epidemiologic data that exposure to ultrafine particles is a significant risk for the development of ischemic heart disease. Thus, the mechanistic insights into the pathophysiological changes associated with NP-EC interaction provide the basis for a better understanding of NP-induced cytotoxicity and therefore of NP-mediated vascular disease.

Acknowledgements

We thank Natalia Halter and Julia Blechinger for excellent technical help and advice. We thank Rudolf Herrmann and Armin Reller for providing nanoparticles (Department of Solid State Chemistry; University of Augsburg, Germany). This work was supported by the Deutsche Forschungsgemeinschaft (DFG) within the project SPP 1313 (SWS NPBIOMEM), SFB/Transregio 23 (SWS TPA9) and DLC (SWS SCHN 474/4-1).

References

[1] Stix G. Little big science. Nanotechnology Sci Am 2001;285:32–7.
[2] Alivisatos AP. Less is more in medicine. Sci Am 2001;285:66–73.
[3] Riehemann K, Schneider SW, Luger TA, Godin B, Ferrari M, Fuchs H. Nanomedicine – challenge and perspectives. Angew Chem Int Ed Engl 2009;48:872–97.
[4] Santra S, Zhang P, Wang K, Tapec R, Tan W. Conjugation of biomolecules with luminophore-doped silica nanoparticles for photostable biomarkers. Anal Chem 2001;73:4988–93.
[5] Hirsch LR, Stafford RJ, Bankson JA, Sershen SR, Rivera B, Price RE, et al. Nanoshell-mediated near-infrared thermal therapy of tumors under magnetic resonance guidance. Proc Natl Acad Sci U S A 2003;100:13549–54.
[6] Bharali DJ, Klejbor I, Stachowiak EK, Dutta P, Roy I, Kaur N, et al. Organically modified silica nanoparticles: a nonviral vector for in vivo gene delivery and expression in the brain. Proc Natl Acad Sci U S A 2005;102:11539–44.

[7] Gemeinhart RA, Luo D, Saltzman WM. Cellular fate of a modular DNA delivery system mediated by silica nanoparticles. Biotechnol Prog 2005;21:532–7.
[8] Venkatesan N, Yoshimitsu J, Ito Y, Shibata N, Takada K. Liquid filled nanoparticles as a drug delivery tool for protein therapeutics. Biomaterials 2005; 26:7154–63.
[9] De Jong WH, Borm PJ. Drug delivery and nanoparticles:applications and hazards. Int J Nanomedicine 2008;3:133–49.
[10] Merget R, Bauer T, Kupper HU, Philippou S, Bauer HD, Breitstadt R, et al. Health hazards due to the inhalation of amorphous silica. Arch Toxicol 2002; 75:625–34.
[11] Pope 3rd CA, Burnett RT, Thurston GD, Thun MJ, Calle EE, Krewski D, et al. Cardiovascular mortality and long-term exposure to particulate air pollution: epidemiological evidence of general pathophysiological pathways of disease. Circulation 2004;109:71–7.
[12] Borm PJ, Kreyling W. Toxicological hazards of inhaled nanoparticles–potential implications for drug delivery. J Nanosci Nanotechnol 2004;4:521–31.
[13] Mills NL, Tornqvist H, Gonzalez MC, Vink E, Robinson SD, Soderberg S, et al. Ischemic and thrombotic effects of dilute diesel-exhaust inhalation in men with coronary heart disease. N Engl J Med 2007;357:1075–82.
[14] Oberdorster G, Oberdorster E, Oberdorster J. Nanotoxicology: an emerging discipline evolving from studies of ultrafine particles. Environ Health Perspect 2005;113:823–39.
[15] Berry JP, Arnoux B, Stanislas G, Galle P, Chretien J. A microanalytic study of particles transport across the alveoli: role of blood platelets. Biomedicine 1977;27:354–7.
[16] Nemmar A, Hoet PH, Vanquickenborne B, Dinsdale D, Thomeer M, Hoylaerts MF, et al. Passage of inhaled particles into the blood circulation in humans. Circulation 2002;105:411–4.
[17] Wagner DD, Frenette PS. The vessel wall and its interactions. Blood 2008;111: 5271–81.
[18] Huck V, Niemeyer A, Goerge T, Schnaeker EM, Ossig R, Rogge P, et al. Delay of acute intracellular pH recovery after acidosis decreases endothelial cell activation. J Cell Physiol 2007;211:399–409.
[19] Goerge T, Barg A, Schnaeker EM, Poppelmann B, Shpacovitch V, Rattenholl A, et al. Tumor-derived matrix metalloproteinase-1 targets endothelial proteinase-activated receptor 1 promoting endothelial cell activation. Cancer Res 2006;66:7766–74.
[20] Spiel AO, Gilbert JC, Jilma B. von Willebrand factor in cardiovascular disease: focus on acute coronary syndromes. Circulation 2008;117:1449–59.
[21] Nemmar A, Nemery B, Hoet PH, Van Rooijen N, Hoylaerts MF. Silica particles enhance peripheral thrombosis: key role of lung macrophage-neutrophil cross-talk. Am J Respir Crit Care Med 2005;171:872–9.
[22] Nemmar A, Hoylaerts MF, Hoet PH, Nemery B. Possible mechanisms of the cardiovascular effects of inhaled particles: systemic translocation and prothrombotic effects. Toxicol Lett 2004;149:243–53.
[23] Hamilton Jr RF, Thakur SA, Holian A. Silica binding and toxicity in alveolar macrophages. Free Radic Biol Med 2008;44:1246–58.
[24] Lin W, Huang YW, Zhou XD, Ma Y. In vitro toxicity of silica nanoparticles in human lung cancer cells. Toxicol Appl Pharmacol 2006;217:252–9.
[25] Park EJ, Park K. Oxidative stress and pro-inflammatory responses induced by silica nanoparticles in vivo and in vitro. Toxicol Lett 2009;184:18–25.
[26] Blechinger J, Herrmann R, Kiener D, Garcia-Garcia FJ, Scheu C, Reller A, et al. Perylene-labeled silica nanoparticles: synthesis and characterization of three novel silica nanoparticle species for live-cell imaging. Small 2010;6: 2427–35.
[27] Goerge T, Niemeyer A, Rogge P, Ossig R, Oberleithner H, Schneider SW. Secretion pores in human endothelial cells during acute hypoxia. J Membr Biol 2002;187:203–11.
[28] Mosmann T. Rapid colorimetric assay for cellular growth and survival: application to proliferation and cytotoxicity assays. J Immunol Methods 1983; 65:55–63.
[29] Haslam G, Wyatt D, Kitos PA. Estimating the number of viable animal cells in multi-well cultures based on their lactate dehydrogenase activities. Cytotechnology 2000;32:63–75.
[30] Schneider SW, Nuschele S, Wixforth A, Gorzelanny C, Alexander-Katz A, Netz RR, et al. Shear-induced unfolding triggers adhesion of von Willebrand factor fibers. Proc Natl Acad Sci U S A 2007;104:7899–903.
[31] Goerge T, Kleineruschkamp F, Barg A, Schnaeker EM, Huck V, Schneider MF, et al. Microfluidic reveals generation of platelet-strings on tumor-activated endothelium. Thromb Haemost 2007;98:283–6.
[32] Even-Ram S, Yamada KM. Cell migration in 3D matrix. Curr Opin Cell Biol 2005;17:524–32.
[33] Peters K, Unger RE, Kirkpatrick CJ, Gatti AM, Monari E. Effects of nano-scaled particles on endothelial cell function in vitro: studies on viability, proliferation and inflammation. J Mater Sci Mater Med 2004;15:321–5.
[34] Liu X, Sun J. Endothelial cells dysfunction induced by silica nanoparticles through oxidative stress via JNK/P53 and NF-kappaB pathways. Biomaterials 2010;31:8198–209.
[35] Nel A, Xia T, Madler L, Li N. Toxic potential of materials at the nanolevel. Science 2006;311:622–7.
[36] Ye YY, Liu JW, Chen MC, Sun LJ, Lan MB. In vitro toxicity of silica nanoparticles in myocardial cells. Environ Toxicol Pharmacol 2010;29:131–7.
[37] Napierska D, Thomassen LC, Rabolli V, Lison D, Gonzalez L, Kirsch-Volders M, et al. Size-dependent cytotoxicity of monodisperse silica nanoparticles in human endothelial cells. Small 2009;5:846–53.
[38] Zhang Y, Hu L, Yu D, Gao C. Influence of silica particle internalization on adhesion and migration of human dermal fibroblasts. Biomaterials 2010;31: 8465–74.
[39] Ravi Kumar MN, Sameti M, Mohapatra SS, Kong X, Lockey RF, Bakowsky U, et al. Cationic silica nanoparticles as gene carriers: synthesis, characterization and transfection efficiency in vitro and in vivo. J Nanosci Nanotechnol 2004;4:876–81.
[40] Chang JS, Chang KL, Hwang DF, Kong ZL. In vitro cytotoxicitiy of silica nanoparticles at high concentrations strongly depends on the metabolic activity type of the cell line. Environ Sci Technol 2007;41:2064–8.
[41] Chen M, von Mikecz A. Formation of nucleoplasmic protein aggregates impairs nuclear function in response to SiO2 nanoparticles. Exp Cell Res 2005; 305:51–62.
[42] Jin Y, Kannan S, Wu M, Zhao JX. Toxicity of luminescent silica nanoparticles to living cells. Chem Res Toxicol 2007;20:1126–33.
[43] Fubini B, Hubbard A. Reactive oxygen species (ROS) and reactive nitrogen species (RNS) generation by silica in inflammation and fibrosis. Free Radic Biol Med 2003;34:1507–16.
[44] Eom HJ, Choi J. Oxidative stress of silica nanoparticles in human bronchial epithelial cell, Beas-2B. Toxicol In Vitro 2009;23:1326–32.
[45] Bombeli T, Karsan A, Tait JF, Harlan JM. Apoptotic vascular endothelial cells become procoagulant. Blood 1997;89:2429–42.
[46] Xu F, Sun Y, Chen Y, Li R, Liu C, Zhang C, et al. Endothelial cell apoptosis is responsible for the formation of coronary thrombotic atherosclerotic plaques. Tohoku J Exp Med 2009;218:25–33.
[47] Serda RE, Gu J, Burks JK, Ferrari K, Ferrari C, Ferrari M. Quantitative mechanics of endothelial phagocytosis of silicon microparticles. Cytometry A 2009;75:752–60.
[48] Serda RE, Gu J, Bhavane RC, Liu X, Chiappini C, Decuzzi P, et al. The association of silicon microparticles with endothelial cells in drug delivery to the vasculature. Biomaterials 2009;30:2440–8.
[49] Nam HY, Kwon SM, Chung H, Lee SY, Kwon SH, Jeon H, et al. Cellular uptake mechanism and intracellular fate of hydrophobically modified glycol chitosan nanoparticles. J Control Release 2009;135:259–67.
[50] Serda RE, Ferrati S, Godin B, Tasciotti E, Liu X, Ferrari M. Mitotic trafficking of silicon microparticles. Nanoscale 2009;1:250–9.
[51] Huang X, Teng X, Chen D, Tang F, He J. The effect of the shape of mesoporous silica nanoparticles on cellular uptake and cell function. Biomaterials 2010;31: 438–48.